

Ribosomal Target-Binding Sites of Antimicrobial Peptides Api137 and Onc112 Are Conserved among Pathogens Indicating New Lead Structures To Develop Novel Broad-Spectrum Antibiotics

Lisa Kolano,^[a, b] Daniel Knappe,^[a, b, c] Daniela Volke,^[a, b] Norbert Sträter,^[a, b] and Ralf Hoffmann^{*[a, b]}

Dedication to Professor *Laszlo Otvos* on the occasion of his 65th birthday.

Proline-rich antimicrobial peptides expressed in insects are primarily active against Enterobacteriaceae. Mechanistically, they target the bacterial (70S) ribosome after partially transporter-based cellular uptake, as revealed for Api137 and Onc112 on *Escherichia coli*. Following molecular modeling indicating that the Onc112 contact site is conserved among the ribosomes of high-priority pathogens, the ribosome binding of Api137 and Onc112 was studied. The dissociation constants (K_d) of Onc112 were ~75 nmol/L for *Escherichia coli*, *Klebsiella pneumoniae*, and *Acinetobacter baumannii*, 36 nmol/L for *Pseu-*

domonas aeruginosa, and 102 nmol/L for *Staphylococcus aureus*, thus indicating a very promising lead structure for developing broad-spectrum antibiotics. Api137 bound weaker with K_d values ranging from 155 nmol/L to 13 μ mol/L. For most bacteria, the antibacterial activities were lower than predicted from the K_d values, which was only partially explained by their ability to enter bacterial cells. Other factors limiting the activity expected from the ribosome binding might be off-target binding.

Introduction

The development of antibiotics was one of the greatest achievements of drug development, which is currently challenged by the global spread of multi- and pan-resistant bacteria.^[1] As new or, more precisely, previously unknown resistance mechanisms spread frequently into clinically relevant pathogens, there is an urgent need for substances using novel modes of action currently not utilized by approved antibiotics. Such a broad reservoir of antibiotics targeting different intracellular structures and membrane components will eventually reduce the risk of treatment failures linked to resistances determined in vitro. Antimicrobial peptides (AMPs), which are


expressed in all kingdoms of life, rely on a huge variety of structures and diverse mechanisms.^[2] Among them are proline-rich AMPs (PrAMPs) expressed in mammals and insects that are primarily active against Gram-negative pathogens.^[3] Insect-derived PrAMPs are around 20 residues long with a proline content of roughly 30%, which provides reasonable proteolytic stability, and at least one Pro-Arg-Pro-motif. Due to the high content of proline and arginine residues, PrAMPs can freely penetrate through the outer membrane that enables their active translocation from periplasmic space to cytosol by transporters SbmA and MdtM.^[4] PrAMPs inhibit bacterial protein expression by targeting the bacterial ribosome either deep in the peptide exit tunnel (oncocin-type binding) blocking the tunnel or at the end of the peptide exit tunnel (apidaecin-type binding) capturing release factors.^[5]


In recent years, we have optimized apidaecin 1b (identified in honeybees) and oncopeltus AMP 4 (expressed in milkweed bugs) for improved antibacterial activities primarily against *Escherichia coli*, *Klebsiella pneumoniae*, and *Pseudomonas aeruginosa*, that is, Api88 and Api137 as well as Onc72 and Onc112 (sequences in Table S1 in the Supporting Information).^[6] These studies considered initially the minimal inhibitory concentration (MIC) as primary criterion for the activity, which was confirmed in different infection models. The identification of the 70S ribosome as primary target^[5a] and consecutive studies providing the structures of Onc112- and Api137-ribosome complexes^[5b-d] allow quantifying the PrAMP-ribosome binding for different bacteria to explore their maximal activity spectrum neglecting medium compositions, which strongly affect the MIC values, as well as the cellular uptake. Dissociation constants (K_d) of Api88,

[a] L. Kolano, Dr. D. Knappe, Dr. D. Volke, Prof. Dr. N. Sträter, Prof. Dr. R. Hoffmann
Faculty of Chemistry and Mineralogy
Institute of Bioanalytical Chemistry
Deutscher Platz 5, 04103 Leipzig (Germany)
E-mail: bioanaly@rz.uni-leipzig.de

[b] L. Kolano, Dr. D. Knappe, Dr. D. Volke, Prof. Dr. N. Sträter, Prof. Dr. R. Hoffmann
Center for Biotechnology and Biomedicine (BBZ)
Deutscher Platz 5, 04103 Leipzig (Germany)

[c] Dr. D. Knappe
EnBiotix GmbH Leipzig
Deutscher Platz 5E, 04103 Leipzig (Germany)

 Supporting information for this article is available on the WWW under <https://doi.org/10.1002/cbic.202000109>

 © 2020 The Authors. Published by Wiley-VCH Verlag GmbH & Co. KGaA. This is an open access article under the terms of the Creative Commons Attribution Non-Commercial NoDerivs License, which permits use and distribution in any medium, provided the original work is properly cited, the use is non-commercial and no modifications or adaptations are made.

Api137, Onc72, and Onc112, which were reported for ribosomes isolated from *E. coli* BL21(DE3)RIL (Table S1) using a fluorescence polarization assay, were 1220 ± 90 , 560 ± 60 , 450 ± 30 , and 90 ± 3 nmol/L, respectively.^[5,7] As ribosomal proteins are highly conserved among bacteria, we hypothesized that

PrAMPs should also bind to ribosomes isolated from other Gram-negative and maybe even from Gram-positive pathogens, although the MIC values of both apidaecin and oncocin analogues vary up to 100-fold among pathogens.

Results and Discussion

The interaction of oncocin with the *Thermus thermophilus* 70S ribosome has been characterized by crystal structure analysis (PDB ID: 4Z8 C^[5b]). The peptide interacts exclusively with the 23S ribosomal RNA (rRNA; Figure 1) and blocks the peptidyl transferase center and the peptide exit tunnel of the ribosome. Specific interactions mostly occur via its N-terminal part. A sequence alignment of 23S rRNA sequences shows that the oncocin binding site of *T. thermophilus* is strictly conserved in several species of human pathogens, i.e., *E. coli* BW25113, *P. aeruginosa* ATCC 27853, *K. pneumoniae* ATCC 10031, *Acinetobacter baumannii* ATCC 15308, and *Staphylococcus aureus* DSM 6247 (Figure 2). The conserved structure of the oncocin-binding site indicated that oncocin and its optimized analogues Onc72 and Onc112 might be able to inhibit protein translation in both Gram-positive and Gram-negative bacteria. Thus, we tested the binding of Onc112 to 70S ribosome preparations obtained from five different bacteria.

The K_d values determined for 5(6)-carboxyfluorescein (Cf)-labeled Onc112 and the 70S ribosome isolated from *E. coli* BW25113 were very similar to the values reported for *E. coli* BL21(DE3)RIL after an incubation time of 90 min (Supplementary material, Table S1).^[7] However, when this ribosome preparation protocol was applied to *P. aeruginosa*, a jellylike highly viscous sample was obtained that was unsuitable for fluorescence polarization measurements. Assuming that the high viscosity was mostly due to the presence of DNA, a DNase digest step was added, besides some other minor changes. The ribosome preparation of *E. coli* BW25113 obtained by the published and new protocols provided similar affinities, that is, K_d values of 36 ± 14 and 75 ± 4 nmol/L for Onc112 and 328 ± 72 and 379 ± 22 nmol/L for Api137 (Figure 3, Tables 1 and S1).^[7] The K_d value of a scrambled Onc112 was eight times higher than for Onc112; this is in agreement with data reported for truncated and inversed peptides.^[5,9]

As we concluded that DNase treatment did not affect the fluorescence polarization assay, the new protocol was applied to all studied bacteria. The K_d values determined for the *K. pneumoniae* ATCC 10031 ribosome and Onc112 ($K_d = 77 \pm$

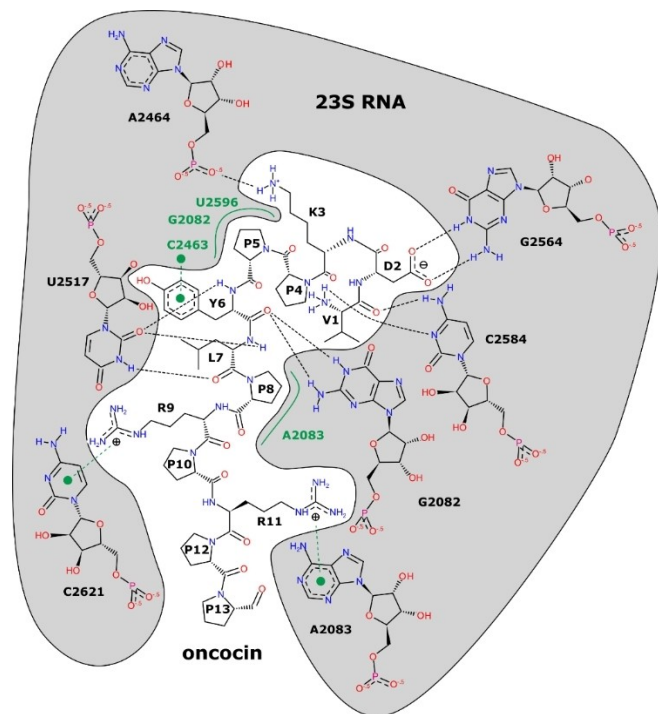


Figure 1. Scheme of the interaction of oncocin with the 23S rRNA of the *T. thermophilus* ribosome. The scheme was generated with PoseView^[6] and edited with inkscape (<http://www.inkscape.org/>).

```

2082 2453 2462 2504 2514          2564 2584 2592 2613 2620
T.t.  CGAC...CCG...AACAG UUG GAUGUCGG...UGUUC...ACG UGGGUUC...CAG...GUCU
S.a.  CGAU...CCG AACAG UUG GAUGUCGG...UGUUC...ACG UGGGUUC...CAG...GUCC
E.c.  UGAU...UCC AACAG UUG GAUGUCGG...UGUUC...ACG UGGGUUU...CAG...GUCC
K.p.  UGAU...UCC AACAG UUG GAUGUCGG...UGUUC...ACG UGGGUUU...CAG...GUCC
P.a.  CGAU...UCC AACAG UUG GAUGUCGG...UGUUC...ACG UGGGUUU...CAG...GUCC
A.b.  UGAU...UCU AACAG UUG GAUGUCGG...UGUUC...ACG UGGGUUU...CAG...GUCC
H.s.  CGAC...CCG AACAG UUG GAUGUCGG...UGUUC...ACG UGGGUUU...CAG...GUU

```

Figure 2. Sequence alignment of 23S rRNA at the oncocin binding site. The residues depicted in bold are within 5 Å of oncocin in the crystal structure of oncocin bound to the *T. thermophilus* ribosome. Residues that interact with oncocin via the base are underlined. Four residues differ in the human 28S rRNA (boxed in red). T.t, *S. aureus*, K. p., *P. aeruginosa*, A.b., and H.s. denote *T. thermophilus*, *Staphylococcus aureus*, *E. coli*, *K. pneumoniae*, *P. aeruginosa*, *A. baumannii*, and *Homo sapiens*, respectively. See Tables S2 and S3 for alignment statistics.

Table 1. Dissociation constants (K_d) and MIC values measured for Api137 and Onc112. K_d values were determined with Cf-labeled Api137 or Onc112 and 70S ribosome preparations obtained from the mentioned bacteria.

| Bacterium | Onc112 K_d [nmol/L] | MIC [mg/L (μ mol/L)] | Api137 K_d [nmol/L] | MIC [mg/L (μ mol/L)] |
|----------------------|-----------------------------|------------------------------|-----------------------------|------------------------------|
| <i>E. coli</i> | 75 ± 4 | 8 (3.4) | 379 ± 22 | 4 (1.8) |
| <i>K. pneumoniae</i> | 77 ± 1 | 2 (0.8) | 155 ± 18 | 2 (0.9) |
| <i>A. baumannii</i> | 73 ± 4 | 32 (13.4) | 2493 ± 196 | 128 (56) |
| <i>P. aeruginosa</i> | 36 ± 2 | 64 (26.8) | 257 ± 8 | > 128 (> 56) |
| <i>S. aureus</i> | 102 ± 5 | 64 (26.8) | 13079 ± 2059 | > 128 (> 56) |

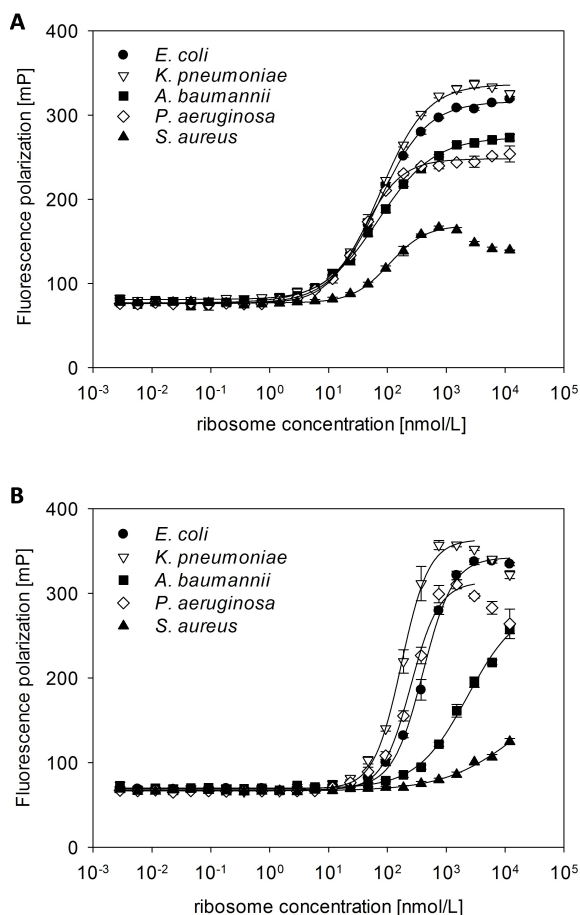


Figure 3. Fluorescence polarization curves recorded for A) Cf-Onc112 (Cf-VDKPPYLPRPRPPRrYr-NH₂, r: D-arginine) or B) Cf-Api137 (gu-O(Cf)NNRPVYIPRPRPPHRL-OH, gu: N, N, N', N'-tetramethylguanidino, O: L-ornithine) in the presence of 70S ribosome preparation obtained from five different bacteria. The data were recorded after an incubation period of 90 min at 28 °C. Curves were fitted to a dose-response curve with a variable slope parameter [$y = \min + (\max - \min) / (1 + (x/IC_{50})^{-\text{Hill slope}})$] by using SigmaPlot.

1 nmol/L) were almost identical to *E. coli*, which was expected as both bacteria belong to the family of Enterobacteriaceae. In agreement with molecular modeling, Onc112 bound equally well to *A. baumannii* ATCC 15308 ribosomes ($K_d = 73 \pm 4$ nmol/L), even better to the ribosome preparation of *P. aeruginosa* ATCC 27853 ($K_d = 36 \pm 2$ nmol/L), and only slightly worse to the ribosome of *S. aureus* DSM 6247 ($K_d = 102 \pm 5$ nmol/L). Both the molecular modeling and the binding affinities determined in vitro indicated a highly conserved binding site of Onc112 among the tested Gram-negative and Gram-positive bacteria (Figure 1, Table 1). Thus, Onc112 represents a highly relevant scaffold to develop antibiotics targeting a broad range of pathogens.

Api137, which binds in reverse direction compared to Onc112 and close to the peptidyl transferase center, bound equally well to the ribosome preparations of both Enterobacteriaceae and *P. aeruginosa* (K_d ranging from 155 to 379 nmol/L; Figure 3, Table 1), but less efficient than Onc112. However, the binding to *A. baumannii* and *S. aureus* ribosomes

was much weaker with K_d values only in the low $\mu\text{mol/L}$ -range. Assuming that the reduced binding constants of Api137 might be related to the release factors participating in its ribosome binding, the tryptic in-gel digests of all five ribosome preparations were analyzed by LC-MS. Release factors were indeed detected in the ribosome preparations of *E. coli* (RF1 and RF3), *P. aeruginosa* (RF1 and RF2), and *K. pneumoniae* (RF1, RF2, and RF3), but not in the digests of *A. baumannii* and *S. aureus* despite detecting similar numbers of other ribosomal proteins (Table S4). However, addition of recombinant *E. coli* RF1 at equimolar quantities to the *A. baumannii* ribosome preparation did not affect the K_d values of Api137. It should be noted that it is uncertain if recombinant *E. coli* RF1 can bind to *A. baumannii* ribosomes and if release factors affect the K_d values of Api137.

The decreasing fluorescence polarization values obtained for Onc112 and *S. aureus* as well as for Api137 and *K. pneumoniae* and *P. aeruginosa* at ribosome concentrations above 1 $\mu\text{mol/L}$ might be explained by proteolytic activity remaining in the ribosome preparations. Even if proteases are present at very low concentrations they might partially cleave the free peptides in the highly concentrated samples. However, the signal intensities observed in MALDI-MS for undiluted samples (3 $\mu\text{mol/L}$ ribosome) after an incubation time of two hours did not indicate a significant peptide loss.

Surprisingly, the similar K_d values measured for Onc112 and partially for Api137 did not fit to the respective antibacterial activities in vitro (Table 1). The MIC values of Onc112 increased fourfold from *K. pneumoniae* to *E. coli* and again fourfold to *A. baumannii*, despite the identical K_d values, and doubled again for *P. aeruginosa* to 64 $\mu\text{g/mL}$, although Onc112 bound the strongest to the *P. aeruginosa* ribosome preparation. Similarly, the K_d values determined for Api137 and the ribosome of *P. aeruginosa* were just in the middle of the values measured for *E. coli* and *K. pneumoniae*, although the MIC was >128 mg/L compared to 4 and 2 $\mu\text{g/mL}$, respectively. This implies that further factors in addition to target binding contribute significantly to the antibacterial activity of both PrAMPs, most likely transport mechanisms used by the studied short PrAMPs. A recent study demonstrated that reduced peptide quantities detected in the supernatant of an *E. coli* culture correspond well to the peptide quantities present in the corresponding cell pellet.^[9] Thus, the cellular uptake of Api137 and Onc112 for a 30-min incubation period was judged from the difference of the peptide quantities measured in a cell-free medium and the medium of a cell culture after centrifugation (supernatant). The envisaged “high-throughput” method for low peptide quantities demanded a sensitive and specific analysis. Thus, a previously reported LC-MS method for the quantification of Api137 and Onc112 in mouse plasma^[10] was adopted to quantify Api137, Onc112, and the corresponding controls, that is, D-Api137 and D-Onc112, in cation-adjusted Muller-Hinton broth (MHB2). The method, which relied on solid phase extraction, RP-HPLC, and multiple reaction monitoring (MRM) on an ESI-QqLIT-MS, provided limits of detection (LODs) of 0.5 $\mu\text{g/mL}$ for Onc112 and 1 $\mu\text{g/mL}$ for Api137 (Tables S5 and S6). The limits of quantification (LOQs) were 0.5 $\mu\text{g/mL}$ and 2 $\mu\text{g/mL}$, respectively.

The bacterial uptake was studied for cultures in 96-well plates containing $\sim 7.5 \times 10^8$, $\sim 7.5 \times 10^9$ (low/high cell counts) or zero cells/mL (MHB2 medium as control). The differences of the peptide quantities determined in the control medium and the supernatants of the cell cultures (30 min incubation period) are referred to as bacterial uptake, which represents the total peptide amount present in the cytosol and either the inner/outer membranes and periplasmic space of Gram-negatives or the cell wall of *S. aureus*. It should be noted that the cell numbers used in the uptake experiments are 1,000 to 10,000 times higher than in the MIC testing. MIC values measured for such high cell numbers would be much higher, that is, > 128 mg/L even for *K. pneumoniae*.

For low cell counts, the supernatants of the Gram-negatives contained between 80 ± 17 and $98 \pm 7\%$ of the L-Onc112 quantities present in the control (Figure 4 A) indicating uptake rates below 20%. Expectedly, lower quantities of typically around 75% were detected in the supernatants of the high cell count experiments, except for *E. coli* with only $56 \pm 7\%$ (Figure 4 B). In view of similar bacterial uptake rates and comparable ribosome affinities measured for four Gram-negatives, the higher antibacterial activities of Onc112 against Enterobacteriaceae compared to non-fermenters *P. aeruginosa* and *A. baumannii* cannot be explained. Even for Enterobacteriaceae, the uptake rates calculated for high cell counts of *E. coli* ($\sim 44\%$) and *K. pneumoniae* ($\sim 25\%$) are opposite to the MIC values of 8 and 2 mg/L, respectively, despite identical ribosome binding affinities. This clearly indicates that lower peptide quantities are required to inhibit the growth of *K. pneumoniae*. Considering the uptake of 352 and 208 ng Onc112 by *E. coli* and *K. pneumoniae* (high cell counts), a single cell contained on average 0.5 and 0.3 fg peptide, respectively. This corresponds

very well to the 0.2 fg/cell recently reported for *E. coli* BL21AI incubated with half of the L-Onc112 concentration (i.e., 4 mg/L).^[9]

The lowest L-Onc112 quantities were present in the supernatants of *S. aureus* cultures, that is, $34 \pm 6\%$ for low and $26 \pm 12\%$ for high cell counts. This high uptake and the strong ribosome binding ($K_d = 102 \pm 5$ nmol/L) indicate a strong activity, which is in contrast to the high MIC value of 64 $\mu\text{g/mL}$. Thus, we quantified the peptides also in the cell pellets to verify the uptake rates calculated from the reduced peptide concentrations in the supernatants. The total quantities of L-Onc112 determined in *S. aureus* supernatants and pellets were around 110%. Similar peptide quantities were calculated for the Gram-negative bacteria (102 to 128%; Figure S3), confirming again that the cellular uptake of Onc112 can be deduced from the concentrations in the supernatants. Furthermore, it clearly indicates that Onc112 was strongly enriched in *S. aureus* and not lost during the experiment, for example by degradation (Figure S3).

The uptake of Api137 for low (high) cell counts of *E. coli* and *A. baumannii* was $83 \pm 7\%$ ($60 \pm 14\%$) and $98 \pm 6\%$ ($90 \pm 10\%$), respectively, which was similar to Onc112 except for the high-cell count experiment with *A. baumannii* (Figure 4C and D). For these two bacteria, the higher uptake rates in *E. coli* and the more than sixfold higher affinity to the *E. coli* ribosome resembled nicely the 32-fold lower MIC values of 4 $\mu\text{g/mL}$ for *E. coli* and 128 $\mu\text{g/mL}$ for *A. baumannii*. The uptake rate in *K. pneumoniae* appeared to be extremely low, as we did not detect reduced peptide concentrations in the supernatants, not even when high cell counts were used ($101 \pm 6\%$). Considering the extremely low uptake, the twofold lower MIC for Api137 against *K. pneumoniae* (2 $\mu\text{g/mL}$) is surprising despite the twofold higher affinity to the ribosome.

For *P. aeruginosa* and Gram-positive *S. aureus* the uptake was high based on the remaining quantities of $40 \pm 4\%$ ($18 \pm 1\%$; below LOQ) and $54 \pm 7\%$ ($26 \pm 11\%$) in low (high) cell count-experiments. Despite this favorable uptake, both species are not susceptible to Api137 (MIC > 128 $\mu\text{g/mL}$), which could be explained for *S. aureus* by a 34-fold higher K_d value, but not for *P. aeruginosa*, as the K_d values were even slightly better than for *E. coli*.

The uptake rates of controls D-Api137 and D-Onc112 were similar to the corresponding L-peptides, except for Api137 and *P. aeruginosa*, indicating no stereospecific effects on the uptake mechanisms. This was generally not surprising as the SbmA transporter was reported to transport structurally diverse AMPs. The different uptake rates of D- and L-Api137 in *P. aeruginosa* were attributed to proteolytic degradation, as the L-Api137 quantities in the pellet were much lower than calculated from the reduced peptide concentrations in the supernatants. Indeed, Api137(8-18) and Api137(9-18) were identified as degradation products by nanoRP-HPLC-ESI-QTOF mass spectrometry (Acquity UPLC, Synapt G2Si MS, Waters, MS Technologies, Manchester, UK; Figure S2). As the cleavage site appears to be after Tyr7 and Ile8, substitution of Ile8 or a backbone modification nearby would reasonably stabilize the peptide and likely increase the activity, if it does not affect the ribosome

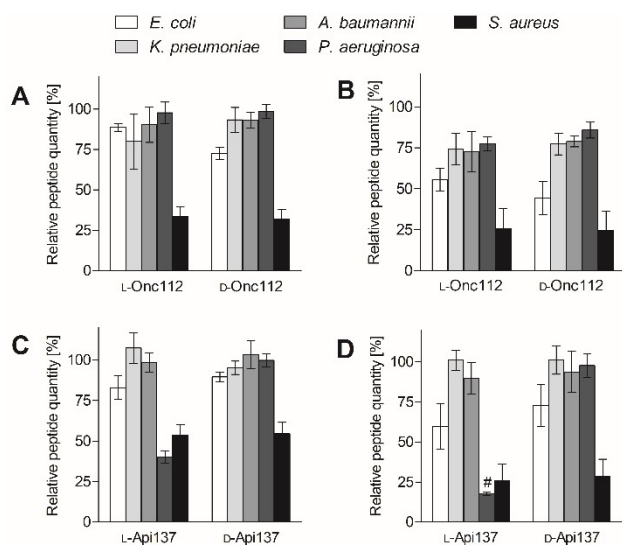


Figure 4. Relative peptide quantities determined for five bacterial cell culture supernatants after an incubation period of 30 min. Cell counts were adjusted by optical density to $\sim 7.5 \times 10^8$ (A,C) and $\sim 7.5 \times 10^9$ cells/mL (B,D). Peptides were quantified by LC-MS using multiple reaction monitoring (MRM). # indicates an Api137 quantity below the LOQ corresponding to 20%. An alternative view of the data is shown in Figure S2.

binding. Indeed, Api795 carrying an Ile8Orn substitution designed in a structure activity relationship study was more active against *Pseudomonas aeruginosa*, especially in full Muller-Hinton broth with MIC values of 8–16 $\mu\text{g}/\text{mL}$.^[11]

As centrifugation does not remove the supernatant completely from the cell pellets, peptide quantities will be overestimated due to the remaining medium volume and the peptide concentration. This is indicated by the Onc112 quantities determined in the pellets and the supernatants of Gram-negatives ranging from 96 ± 15 to $163 \pm 4\%$ (Figures S3 and S4). The medium could be washed out from the cell pellets with buffer, but this may also wash out peptides from the cells leading to an underestimation.

It has to be noted that it remains an open question, how the uptake rates calculated here have to be interpreted mechanistically, as it is unknown what portion entered the cytosol and finally reached the ribosomes. For Gram-negatives, the peptides are likely partially trapped in membranes, the periplasmic space, and at the negatively charged surface. Such off-target effects will most likely differ among bacteria and are thus difficult to study. However, at least for Api88 – a C-terminally amidated version of Api137 – we showed in 2012 that it enters *E. coli*, *K. pneumoniae*, and *P. aeruginosa* at reasonable quantities when N-terminally labeled with carboxy-fluorescein (Cf; Figures 2 and S3^[6c]). Confocal laser scanning microscopy indicated further that Cf-Api88 enters the cytoplasm for all three bacteria. However, PrAMPs will likely bind to other intracellular proteins as well. Recently, we reported that Api88, a close analogue of Api137, binds in vivo to nonribosomal proteins, such as DnaK and GroEL.^[12] DnaK was identified as an intracellular target of PrAMPs including apidaecins and oncocins,^[13] but the binding is much weaker than for ribosomes.

Similar off-target effects can be assumed for *S. aureus*, as cationic AMPs strongly interact with anionic teichoic acids in the cell wall. Teichoic acids may guide AMPs to the cytoplasmic membrane,^[14] but might also trap Api137, Onc112, and other PrAMPs. This could explain why high quantities of Onc112 and Api137 were detected in the cell pellets without inhibiting cell growth, although Onc112 binds strongly to the ribosome.

Independent of the mode of action, cellular uptake, and likely off-target effects of Api137 and Onc112, this study strongly supports the initial hypothesis that Onc112 is a very promising lead compound as it binds very strongly to the ribosomes of at least four high-priority Gram-negative pathogens and Gram-positive *S. aureus* and most likely inhibits protein translation. Thus, it represents a universal lead structure for developing broadband antibiotics. This broad activity spectrum assumed from the K_d values is supported by experimental data presented in the first publication about oncocins and their antibacterial activity.^[12] The authors showed that Onc72 and Api88 are highly active against a broad panel of 37 clinical isolates of *E. coli*, *K. pneumoniae*, *P. aeruginosa*, *A. baumannii*, *Enterobacter cloacae*, and *Proteus vulgaris* with MIC values ranging from 0.125 to 8 mg/L.^[5c,12] It is tempting to speculate that the standard MIC-testing conditions indicating that pathogens like *P. aeruginosa* are resistant against PrAMPs

are inappropriate for evaluating the antibiotic potential of PrAMPs and maybe more general for AMPs targeting intracellular bacterial structures. It might be better to evaluate the “maximal” antibiotic activity spectrum using unfavorable bacterial growth conditions, such as low medium strength, and then optimize the lead compounds based providing incrementally increasing culture conditions or in vivo tests. In this respect, standard MIC-testing may have prevented thorough AMP-drug development efforts in the past.

Conclusion

PrAMPs including Api137 and Onc112 are primarily active against Enterobacteriaceae, while other Gram-negative pathogens are less susceptible and Gram-positive bacteria appear to be resistant. We could show that this limitation is not due the target binding, as Onc112 bound strongly with K_d values in the low-nanomolar region to the ribosomes isolated from five different clinically relevant bacteria including *S. aureus*. The conserved target should allow the development of novel broadband antibiotics based on the pharmacophore unit of Onc112. Interestingly, the observed MIC values could neither be explained by the target binding nor the cellular uptake indicating that further factors have to be considered for future drug development efforts, such as off-target binding.

Experimental Section

Materials: AppliChem GmbH (Darmstadt, Germany): HEPES ($\geq 99.5\%$); Carl Roth GmbH & Co. (Karlsruhe, Germany): lysogeny broth (LB) Miller, nutrient broth, agar-agar (Kobe I); Honeywell FlukaTM (Seelze, Germany): MgCl_2 ($\geq 99\%$), NH_4Cl ($\geq 99.8\%$); EMD Millipore Calbiochem[®] (Darmstadt, Germany): Casein ($\geq 95\%$); Sigma Aldrich (Steinheim, Germany): 5(6)-carboxyfluorescein (Cf, for fluorescence), disodium hydrogen phosphate-12 H_2O ($\geq 99\%$), Mueller-Hinton broth 2 (MHB2, for microbiology, cation-adjusted), NaCl ($\geq 99.5\%$), trifluoroacetic acid (TFA, for HPLC, $\geq 99\%$), potassium dihydrogen phosphate ($\geq 99\%$), KOH ($> 90\%$), 2-mercaptoethanol ($\geq 99\%$); meropenem trihydrate ($\geq 98\%$); Thermo Fisher Scientific Inc. (Darmstadt, Germany): DNase I (RNase-free, 1 $\text{u}/\mu\text{L}$); VWR International S. A. S. (Fontenay-sous-Bois, France): acetonitrile (HPLC-gradient grade); formic acid ($\sim 98\%$); Serva Electrophoresis GmbH (Heidelberg, Germany): Tween[®] 20 (pure).

Water was purified on a Purelab Ultra water purification system (electrical resistivity $> 182 \text{ k}\Omega\text{-m}$; organic content $< 2 \text{ ppb}$; ELGA LabWater, Celle, Germany).

The following bacteria were used: *Escherichia coli* BW25113 (lacI^q rrnB3 Δ lacZ4787 hsdR514 DE(araBAD)567 DE(rhaBAD)568 rph-1, Keio collection), *Pseudomonas aeruginosa* DSM 1117 / ATCC[®] 27853TM, *Klebsiella pneumoniae* DSM 681 / ATCC[®] 10031TM, *Acinetobacter baumannii* DSM 30008 / ATCC[®] 15308TM, *Staphylococcus aureus* DSM 6247 (DSMZ – German Collection of Microorganisms and Cell Cultures, Braunschweig, Germany).

Synthesis: Peptides were synthesized by Fmoc/tBu-chemistry on Rink amide or Wang resins and purified by RP-HPLC using an acetonitrile gradient in the presence of 0.1% TFA.^[6a,d] The masses were confirmed by MALDI- and ESI-MS and the purities were determined by RP-HPLC recording the absorbance at 214 nm. For

fluorescence polarization, 5(6)-carboxyfluorescein was coupled to the N-terminus of Onc112 and Api137.^[6a]

Preparation of 70S ribosomes: The previously reported 70S ribosome protocol was slightly modified.^[5a,15] Briefly, bacteria were cultured in LB overnight (37 °C, 5 mL), transferred to fresh LB medium (500 mL) to establish a logarithmic growth phase, and cultured using LB medium (3 L, 37 °C) for *E. coli*, *K. pneumoniae* (8 L), *A. baumannii* (8 L), *P. aeruginosa* (8 L), and *S. aureus* (22 L). Bacteria were harvested at an OD₆₀₀ of around 1 by centrifugation (5000 g, 15 min, 4 °C, centrifuge Avanti JXN-26, rotor JA-10, Beckman Coulter, Krefeld, Germany), and the pellets were stored at –80 °C. The frozen cells were suspended in HEPES buffer (2 mL/g cells, 20 mmol/L HEPES, 30 mmol/L NH₄Cl, 6 mmol/L MgCl₂, 4 mmol/L 2-mercaptoethanol, pH 7.6; room temperature). The cell suspension was disrupted with a bead mill homogenizer (BeadBeater, BioSpec Products, Inc., Bartlesville, OK, USA) using zirconia/silica beads (0.1 mm diameter, BioSpec Products, Inc., Bartlesville, OK USA) in five intervals of one minute each. The lysates were incubated with DNase I (5 U/mL) and meropenem (280 mg/L) for one hour on ice to digest DNA and to kill bacteria surviving the homogenization procedure, respectively. The cell debris was removed by centrifugation (16000 g, 30 min, 4 °C, afterwards 32000 g, 60 min, 4 °C, Avanti JXN-26, JA-14.50, Beckman Coulter, Krefeld, Germany) and the supernatant was stored at –80 °C. The ribosome was pelleted by ultracentrifugation of the supernatant (165000 g, 17 h, 4 °C). The pellet was suspended in HEPES buffer (0.05–0.1 mL/g cell pellet) and stored at –80 °C. The ribosome concentration was measured by recording the absorbance of RNA at 260 nm and considering that 1 AU corresponds to a ribosome concentration of 28 pmol/mL. The molecular weight of the 70S ribosome was assumed to be 2.3 MDa.

Fluorescence polarization assay: Dissociation constants (K_d) were determined in black 384-well plates (flat bottom; ref. 781209, Greiner Bio-One GmbH, Frickenhausen, Germany).^[5a] Wells were blocked with casein (0.5%, w/v) in phosphate buffered saline (PBST; 8.8 mmol/L Na₂HPO₄ × 12 H₂O, 1.2 mmol/L KH₂PO₄, 0.3 mol/L NaCl, pH 7.4 and 0.05% (w/v) Tween® 20) at 4 °C overnight and washed three times with PBST. The 70S ribosome was added in a twofold dilution series in HEPES buffer (20 mmol/L HEPES, 30 mmol/L NH₄Cl, 6 mmol/L MgCl₂, 4 mmol/L 2-mercaptoethanol, pH 7.6, 4 °C) in 23 steps from 12 μmol/L to 2.9 pmol/L (20 μL). The 5(6)-carboxyfluorescein-labeled peptide (20 μL/well, 40 nmol/L) was added, the plate incubated for 90 min (28 °C, dark), and the fluorescence polarization was recorded (λ_{ex} = 485 nm, λ_{em} = 535 nm, microplate reader PARADIGM™, Beckman Coulter, Krefeld, Germany). Dissociation constants (K_d) were calculated by fitting the data from at least two experiments performed in triplicates on different days to a dose-response curve with a variable slope parameter [$y = \min + (\max - \min) / (1 + (x / K_d)^{-\text{Hill slope}})$] using SigmaPlot 13 (Systat Software Inc., San Jose, CA, USA). Each assay was performed in triplicates and repeated at least once on another day.

Antimicrobial activity: Minimal inhibitory concentrations (MICs) were determined in triplicates using a liquid broth micro dilution assay in sterile 96-well plates (polystyrene F-bottom; ref. 655180, Greiner Bio-One GmbH, Frickenhausen, Germany) and a total volume of 100 μL/well. Aqueous peptide solutions (3 g/L) were serially twofold diluted in 25% Mueller-Hinton broth 2 (25% MHB2; 5.5 g/L) starting at a concentration of 128 μg/mL in eight steps (50 μL per well). Overnight cultures of bacteria grown in 25% MHB2 were diluted 30-fold in fresh 25% MHB2. After an incubation period of 4 h (37 °C, 200 rpm), cells were diluted to 1.5 × 10⁷ cfu/mL, based on a McFarland test, and 50 μL were added to each well (final concentration 7.5 × 10⁶ cfu/mL). The plates were incubated at 37 °C for 20 ± 2 h. Optical density was determined at 595 nm using a microplate reader (PARADIGM™, Beckman Coulter, Krefeld, Ger-

many) and the MIC was defined as the lowest peptide concentration preventing visible bacterial growth.

Bacterial uptake: Bacteria were cultured in 25% MHB2 at 37 °C overnight (5 mL), 30-fold diluted in 25% MHB2, and incubated (37 °C, 4.0 ± 0.25 h). The cell density (cfu/mL) was calculated by the optical density recorded at 600 nm (OD₆₀₀) and a McFarland Standard (bioMérieux® Deutschland GmbH, Nürtingen, Germany) assuming that an OD₆₀₀ of 1.0 corresponds to 1.2 × 10⁹ cfu/mL. An aliquot of the cell culture (40 mL) was centrifuged (4 °C, 10 min, 4,000 × g) and the pellet was suspended in 25% MHB2 to obtain a cell density of 1.5 × 10¹⁰ cfu/mL. An aliquot of this cell suspension (0.3 mL) was diluted with 25% MHB2 (2.7 mL) to obtain a cell density of 1.5 × 10⁹ cfu/mL. Aliquots (50 μL) of both cell suspensions were mixed with an equal volume of 25% MHB2 containing a peptide (16 μg/mL) in sterile polystyrene 96-well V-bottom plates (ref. 651180, Greiner Bio-One GmbH, Frickenhausen, Germany). After incubation (30 min, 37 °C, 750 rpm; Thermomixer, Eppendorf AG, Hamburg, Germany or Titramax 1000 Incubator 1000, Heidolph Instruments, Schwabach, Germany) aliquots (10 μL) of the cell suspension were taken to determine the cell counts. The plates were centrifuged (4 °C, 5 min, 1200 g) and 50 μL of the supernatant was removed for quantification of the remaining peptide. The aliquots (10 μL) of the cell suspension were diluted with 0.9% (w/v) sodium chloride (90 μL) and were spread on a nutrient agar plate (10 cm, 50 μL per half plate) to obtain 10 to 100 colonies for a given dilution step. The number of viable cells was determined by counting the colonies after incubation under aerobic conditions overnight (37 °C). Each experiment was done in triplicate and repeated at least once on another day.

Peptide quantification by RP-HPLC-ESI-QqLIT-MS: Medium supernatants (50 μL) were mixed with an equal volume of aqueous TFA (0.2% v/v), further diluted with aqueous TFA (0.1% v/v; 150 μL), and stored on ice (30 min). Samples were purified by solid-phase extraction (SPE; Oasis HLB 96-well Plate, 5 mg sorbent per well, particle size 30 μm, Waters GmbH, Eschborn, Germany). Briefly, the sorbent was conditioned with 500 μL acetonitrile and 500 μL aqueous acetonitrile (40%, v/v) containing formic acid (0.1%, v/v) and equilibrated with 500 μL aqueous TFA (0.1%, v/v; eluent A1). Samples (230 μL) were loaded on the SPE-plate followed by two washings steps (1 mL of eluent A1) and two elution steps with 150 μL aqueous acetonitrile (30%, v/v) containing formic acid (0.1%, v/v) each. The combined eluates were stored at –20 °C.

Samples were dried in a vacuum centrifuge (45 °C; SpeedVac, Thermo Fisher Scientific, Darmstadt, Germany), dissolved in 80 μL of aqueous acetonitrile (3% v/v) containing formic acid (0.1% v/v), and sonicated in an ultrasonic bath for 5 min (Bandelin electronic GmbH & Co. KG, Berlin, Germany). After centrifugation, aliquots (50 μL) were analyzed on the Jupiter C₁₈ column (i.d. 1 mm, length 150 mm, particle size 5 μm, pore size 300 Å; Phenomenex® Inc., Torrance, CA, USA). Elution was achieved by a linear 10-min gradient from 9% to 27% acetonitrile using water (eluent A) and acetonitrile (eluent B), both containing formic acid (0.1% v/v) and a column temperature of 55 °C on an Alliance® 2695 HPLC system. Peptides were quantified by ESI-QqLIT-MS/MS (4000 QTrap®; ABSciex, Darmstadt, Germany) coupled on-line based on a multiple reaction monitoring (MRM) method reported^[10] using slight modifications (Supplement, Table S6). The peptide quantities were calculated relative to peptide quantities determined in control samples (no bacteria, 8 μg/mL) and a calibration curve of the peptide in 25% MHB2 on the same plate.

Analysis of tryptic in-gel digest by nanoRP-HPLC-ESI-QTOF-MS^E: Tryptic peptides were reconstituted in 20 μL of aqueous acetonitrile (3%, v/v) containing formic acid (0.1%, v/v; solvent A). An aliquot (2 μL) was mixed with 13 μL of solvent A and yeast enolase digest

(5 μ L, Waters GmbH, Eschborn) dissolved in solvent A and analyzed.^[16] Data were processed with the Protein Lynx Global Server Software (Version 3.0.3, Waters GmbH, Eschborn). FASTA files were downloaded on August 16th, 2019 (www.uniprot.org/) for *E. coli* (949,991 entries), *K. pneumoniae* (403,196 entries), *A. baumannii* (304,054 entries), *P. aeruginosa* (271,348 entries), and *S. aureus* (186,298 entries) and the yeast enolase sequence added to each FASTA file. Further settings were two missed cleavage sites, trypsin_p as “digester reagent” (cleavage after Arg and Lys even Pro follows), methionine oxidation and cysteine carbamidomethylation as variable modifications. Proteins with at least three identified peptides were considered as identified.

Acknowledgements

This work was supported by the European Fund for Regional and Structure Development (EFRE, EU, and Free State of Saxony; Grant Numbers 100275133 and 100307188). We thank Anna Gallinat and Sontje Krupka for technical assistance.

Keywords: 70S ribosome · antimicrobial peptides · apidaecin · fluorescein polarization · oncocin

- [1] M. Sprenger, *Bull. W. H. O.* **2016**, *94*, 638–639.
- [2] a) E. F. Haney, S. C. Mansour, R. E. Hancock, *Methods Mol. Biol.* **2017**, *1548*, 3–22; b) K. Lohner, K. Hilpert, *Biochim. Biophys. Acta* **2016**, *1858*, 915–917.
- [3] W. Li, J. Tailhades, N. M. O'Brien-Simpson, F. Separovic, L. Otvos, Jr., M. A. Hossain, et al., *Amino Acids* **2014**, *46*, 2287–2294.
- [4] a) M. Mattiuzzo, A. Bandiera, R. Gennaro, M. Benincasa, S. Pacor, N. Antcheva, M. Scocchi, *Mol. Microbiol.* **2007**, *66*, 151–163; b) A. Krizsan, D. Knappe, R. Hoffmann, *Antimicrob. Agents Chemother.* **2015**, *59*, 5992–5898.
- [5] a) A. Krizsan, D. Volke, S. Weinert, N. Sträter, D. Knappe, R. Hoffmann, *Angew. Chem. Int. Ed.* **2014**, *53*, 12236–12239; b) R. N. Roy, I. B. Lomakin, M. G. Gagnon, T. A. Steitz, *Nat. Struct. Mol. Biol.* **2015**, *22*, 466–469; c) A. C. Seefeldt, F. Nguyen, S. Antunes, N. Pérébasquine, M. Graf, S. Arenz, et al., *Nat. Struct. Mol. Biol.* **2015**, *22*, 470–475; d) T. Florin, C. Maracci, M. Graf, P. Karki, D. Klepacki, O. Berninghausen, et al., *Nat. Struct. Mol. Biol.* **2017**, *24*, 752–757.
- [6] a) D. Knappe, S. Piantavigna, A. Hansen, A. Mechler, A. Binas, O. Nolte, L. L. Martin, R. Hoffmann, *J. Med. Chem.* **2010**, *53*, 5240–5247; b) D. Knappe, N. Kabankov, R. Hoffmann, *Int. J. Antimicrob. Agents* **2010**, *37*, 166–170; c) P. Cziala, D. Knappe, F. Fritsche, M. Zahn, N. Berthold, S. Piantavigna, et al., *ACS Chem. Biol.* **2012**, *7*, 1281–1291; d) N. Berthold, P. Cziala, S. Fritsche, U. Sauer, G. Schiffer, D. Knappe, G. Alber, R. Hoffmann, *Antimicrob. Agents Chemother.* **2013**, *57*, 402–409.
- [7] A. Krizsan, C. Prah, T. Goldbach, D. Knappe, R. Hoffmann, *ChemBioChem* **2015**, *16*, 2304–2308.
- [8] K. Stierand, M. Rarey, *ChemMedChem* **2007**, *2*, 853–860.
- [9] L. Holfeld, R. Hoffmann, D. Knappe, *Anal. Bioanal. Chem.* **2017**, *409*, 5581–5592.
- [10] a) R. Schmidt, E. Ostorhazi, F. Wende, D. Knappe, R. Hoffmann, *J. Antimicrob. Chemother.* **2016**, *71*, 1003–1011; b) R. Schmidt, D. Knappe, E. Wende, E. Ostorhazi, R. Hoffmann, *Front. Chem.* **2017**, *5*, 15.
- [11] M. E. C. Bluhm, V. A. F. Schneider, I. Schäfer, S. Piantavigna, T. Goldbach, D. Knappe, P. Seibel, L. L. Martin, E. J. A. Veldhuizen, R. Hoffmann *Front. Cell Dev. Biol.* **2016**, *4*, 39.
- [12] D. Volke, A. Krizsan, N. Berthold, D. Knappe, R. Hoffmann, *J. Proteome Res.* **2015**, *14*, 3274–3283.
- [13] a) G. Kragol, S. Lovas, G. Varadi, B. A. Condie, R. Hoffmann, L. Otvos Jr., *Biochemistry* **2001**, *40*, 3016–3026; b) M. Zahn, N. Berthold, B. Kieslich, D. Knappe, R. Hoffmann, N. Sträter, *J. Mol. Biol.* **2013**, *425*, 2463–2479; c) D. Knappe, M. Zahn, U. Sauer, G. Schiffer, N. Sträter, R. Hoffmann, *ChemBioChem* **2011**, *12*, 874–876.
- [14] N. Malanovic, K. Lohner, *Pharmaceuticals* **2016**, *9*, pii: E59.
- [15] T. Goldbach, D. Knappe, C. Reinsdorf, T. Berg, R. Hoffmann, *J. Pept. Sci.* **2016**, *22*, 592–599.
- [16] F. Fingas, D. Volke, P. Bielefeldt, R. Hassert, R. Hoffmann, *Viro. J.* **2018**, *15*, 1–11.

Manuscript received: February 25, 2020
 Accepted manuscript online: April 15, 2020
 Version of record online: June 30, 2020